ornl

OAK
RIDGE
NATIONAL
LABORATORY

UNION
CARBIDE

NUREG/CR-2299, Vol. 4
(ORNL/TM-8307)

cy. 35

Aerosol Release and Transport Program Quarterly Progress Report for October–December 1981

R. E. Adams M. L. Tobias

ORNL INFORMATION DIVISION
TECHNICAL LIBRARY
Document Reference Section
Building 9711-1, Y-12
LOAN COPY ONLY

Do NOT transfer this document to any other person. If you want others to see it, attach their names,. return the document, and the Library will arrange the loan as requested.

UCN-1624 (3 12-79)

Prepared for the U.S. Nuclear Regulatory Commission
Office of Nuclear Regulatory Research
Under Interagency Agreements DOE 40-551-75 and 40-552-75

OPERATED BY
UNION CARBIDE CORPORATION
FOR THE UNITED STATES
DEPARTMENT OF ENERGY

Printed in the United States of America. Available from
National Technical Information Service
U.S. Department of Commerce
5285 Port Royal Road, Springfield, Virginia 22161

Available from

GPO Sales Program
Division of Technical Information and Document Control
U.S. Nuclear Regulatory Commission
Washington, D.C. 20555

This report was prepared as an account of work sponsored by an agency of the United States Government. Neither the United States Government nor any agency thereof, nor any of their employees, makes any warranty, express or implied, or assumes any legal liability or responsibility for the accuracy, completeness, or usefulness of any information, apparatus, product, or process disclosed, or represents that its use would not infringe privately owned rights. Reference herein to any specific commercial product, process, or service by trade name, trademark, manufacturer, or otherwise, does not necessarily constitute or imply its endorsement, recommendation, or favoring by the United States Government or any agency thereof. The views and opinions of authors expressed herein do not necessarily state or reflect those of the United States Government or any agency thereof.

NUREG/CR-2299, Vol. 4
ORNL/TM-8307
Dist. Category R7

Contract No. W-7405-eng-26

Engineering Technology Division

AEROSOL RELEASE AND TRANSPORT PROGRAM QUARTERLY PROGRESS REPORT FOR OCTOBER–DECEMBER 1981

R. E. Adams M. L. Tobias

Manuscript Completed — April 21, 1982
Date Published — May 1982

NOTICE This document contains information of a preliminary nature. It is subject to revision or correction and therefore does not represent a final report.

Prepared for the
U.S. Nuclear Regulatory Commission
Office of Nuclear Regulatory Research
Under Interagency Agreements DOE 40-551-75 and 40-552-75

NRC FIN No. B0121

Prepared by the
OAK RIDGE NATIONAL LABORATORY
Oak Ridge, Tennessee 37830
operated by
UNION CARBIDE CORPORATION
for the
DEPARTMENT OF ENERGY

CONTENTS

Page

FOREWORD v

SUMMARY vii

GLOSSARY OF ACRONYMS ix

ABSTRACT 1

1. INTRODUCTION 1

2. EXPERIMENTAL PROGRAM 3

2.1 Source Term Experiments in FAST/CRI-III 3

2.1.1 Introduction 3
2.1.2 Discussion of FAST under-sodium test results 4

2.2 Secondary Containment Aerosol Studies in the NSPP 6

2.2.1 Introduction 6
2.2.2 LWR aerosol experiment No. 406 7
2.2.3 LWR aerosol experiment No. 501 10

2.3 Basic Aerosol Experiments in CRI-II 12

2.3.1 Introduction 12
2.3.2 Characterization of the aerosols of cadmium metal and CdO 13

2.4 Core-Melt Aerosol Release and Transport 15

2.4.1 Introduction 15
2.4.2 Observations on the silver alloy control rod interaction with fuel cladding 15

3. ANALYTICAL PROGRAM 26

3.1 Modeling Bubble Oscillations Including Effects of Inertia of the Surrounding Fluid 26

3.1.1 Introduction 26
3.1.2 Differential equations of the system 27
3.1.3 Some results obtained with the code 28

3.2 Analytical Studies with the UVABUBL Code 28

REFERENCES 31

FOREWORD

This report summarizes progress under the Aerosol Release and Transport (ART) Program [sponsored by the Division of Accident Evaluation of the Nuclear Regulatory Commission's (NRC's) Office of Nuclear Regulatory Research] for the period October–December 1981.

Work on this program was initially reported as Volume III of a four-volume series entitled *Quarterly Progress Report on Reactor Safety Programs Sponsored by the NRC Division of Reactor Safety Research*. Prior reports of this series are

Report No.	Period covered
ORNL/TM-4655	April–June 1974
ORNL/TM-4729	July–September 1974
ORNL/TM-4805	October–December 1974
ORNL/TM-4914	January–March 1975
ORNL/TM-5021	April–June 1975

Beginning with the report covering the period July–September 1975 through the report for the period July–September 1981, work under this program was reported as *LMFBR Aerosol Release and Transport Program Quarterly Progress Report*. Prior reports under this title are

Report No.	Period covered
ORNL/NUREG/TM-8	July–September 1975
ORNL/NUREG/TM-9	October–December 1975
ORNL/NUREG/TM-35	January–March 1976
ORNL/NUREG/TM-59	April–June 1976
ORNL/NUREG/TM-75	July–September 1976
ORNL/NUREG/TM-90	October–December 1976
ORNL/NUREG/TM-113	January–March 1977
ORNL/NUREG/TM-142	April–June 1977
ORNL/NUREG/TM-173	July–September 1977
ORNL/NUREG/TM-193	October–December 1977
ORNL/NUREG/TM-213	January–March 1978
ORNL/NUREG/TM-244	April–June 1978
ORNL/NUREG/TM-276	July–September 1978
ORNL/NUREG/TM-318	October–December 1978
ORNL/NUREG/TM-329	January–March 1979
ORNL/NUREG/TM-354	April–June 1979
ORNL/NUREG/TM-376	July–September 1979
ORNL/NUREG/TM-391	October–December 1979
ORNL/NUREG/TM-416	January–March 1980
ORNL/NUREG/TM-417	April–June 1980
ORNL/TM-7806	July–September 1980
ORNL/TM-7884	October–December 1980
ORNL/TM-7946	January–March 1981
ORNL/TM-7974	April–June 1981
ORNL/TM 8149	July–September 1981

Beginning with the report covering the period October–December 1981, work under the program is being reported as *Aerosol Release and Transport Quarterly Progress Report*. Copies of all these reports are available from the Technical Information Center, Oak Ridge, Tennessee 37830.

SUMMARY

M. L. Tobias

The Aerosol Release and Transport (ART) Program at Oak Ridge National Laboratory (ORNL) is designed to investigate the release, transport, and behavior of aerosols which may carry radionuclides originating from a severe accident resulting in core melting. Aspects of the program apply to both light-water reactors (LWRs) and liquid-metal fast breeder reactors (LMFBRs). The experimental programs are being conducted in the Fuel Aerosol Simulant Test (FAST) Facility [which also includes the Containment Research Installation-III (CRI-III) vessel], the Nuclear Safety Pilot Plant (NSPP) Facility, and the CRI-II Facility. The analytical efforts are designed to support the experiments and to provide an independent assessment of the safety margins that exist for the estimation of the radiological consequences of a core meltdown accident.

During this quarter three under-sodium capacitor discharge vaporization tests were performed in FAST to determine appropriate procedures and measurement techniques in a high-temperature sodium environment. Successful vaporization of pellet stacks was achieved, and pressure measurements were made in both the argon cover gas and in the vicinity of the sample itself. Bubble oscillation periods were found significantly shorter than in underwater tests. Argon cover-gas sampling indicated that about 3×10^{-3}% of the UO_2 in the original pellet stack had reached the surface. Sectioning of a sample from a "preheat-only" test indicated about 50% of the pellets became molten at a 1600-W preheat level. The final under-sodium vaporization test produced a pressure spike that may possibly have been a fuel-coolant interaction.

Results from experiment Nos. 406 and 501 in the NSPP are reported. These experiments are part of a series of tests related to aerosol behavior under LWR accident conditions. Experiment No. 406, like the earlier run No. 404, was designed to observe the influence of forced-mixing on an atmosphere of U_3O_8 aerosol in steam. As before, an accelerated rate of removal of aerosol mass occurred during the first hour compared with that observed in Run 403 where no fan-mixer was used. However, after about 1.5 h, the rate of aerosol disappearance appears to be the same in all three experiments even though the fan continued to run. In experiment 501, the object was to observe the influence of condensing steam on an Fe_2O_3-particle aerosol, intended to simulate those that might be generated from core support and structural materials. The aerosol was produced by a plasma torch generator. The maximum concentration of Fe_2O_3 measured was 0.91 $\mu g/cm^3$. In both Test 406 and 501, aerodynamic mass median diameters were measured by both impactor and centrifuge samplers. Scanning electron microscope pictures of the aerosols show similar spherical clumps. Primary particle sizes for Fe_2O_3 appear to be much smaller than those for U_3O_8.

In the program of basic aerosol experiments in the CRI-II Facility, aerosols of cadmium and CdO were generated by plasma torch. Both aerosols displayed a somewhat high aerodynamic mass median diameter and a narrow size distribution. The oxide aerosol appears to be made up of crystalline primary particles in a chain agglomerate while the photomicrographs of the

metal show mainly spherical particles. These observations correspond to distinct differences in measurements of the time variation of airborne concentrations and of size distributions.

In the core-melt experimental program, a representative pressurized-water reactor (PWR) control rod alloy contained in stainless steel tubing was heated in a resistance furnace to 1405°C. The stainless steel tube burst due to the pressure exerted by cadmium vapor, confirming Hagen's observations. In core-melt Test 14, Zircaloy-clad fuel capsules were heated in steam to about 1800°C. This resulted in a "candling" effect with the fuel left standing and the metallic components collapsed into a solid base. In subsequent experiments, a fuel bundle was heated to successive temperatures of 1800, 2200, and 2400°C for approximately equal intervals of time. Measurements of volatile material releases were made by x-ray fluorescence analysis. These showed about half the cadmium had been volatilized but practically no tin or uranium.

In the analytical program, a piston-oscillation code, which models the effect of fluid flow around an expanding or contracting bubble by connecting the upper and lower fluid regions by a pipe of fixed length, was developed. The results obtained for oscillation periods appear, on the basis of the few calculations done, to be quite similar to those obtained without including fluid bypass. The upward motion of the bubble was found to be seriously affected by the inertial effects of the liquid. A side calculation of the properties of the UO_2 vapor indicated it could be considered as essentially an ideal gas with a γ-value of about 1.

The UVABUBL code was modified to include a piston-type expansion process to replace the Rayleigh equations originally used in the code. Thirty-five calculations were done to analyze the FAST water tests using this model, and the agreement with experimental measurements of the period was much improved. In a comparison with an under-sodium test, the code predicts a period of 34 ms vs a measured value of 27 ms. Calculations were also done for a full-size reactor case. The importance of radiative emissivity on condensation rate was again noted.

GLOSSARY OF ACRONYMS

ACRR	Annular Core Research Reactor
AMMD	aerodynamic mass median diameter
ART	Aerosol Release and Transport
BET	Brunauer-Emmet-Teller method
BWR	boiling-water reactor
CDA	core-disruptive accident
CDV	capacitor discharge vaporization
CRBR	Clinch River Breeder Reactor
CRI	Containment Research Installation
CSTF	Containment Systems Test Facility
FAST	Fuel Aerosol Simulant Test
GSD	geometric standard deviation
HCDA	hypothetical core-disruptive accident
LANL	Los Alamos National Laboratory
LMFBR	Liquid-Metal Fast Breeder Reactor
LWR	light-water reactor
NRC	Nuclear Regulatory Commission
NSPP	Nuclear Safety Pilot Plant
ORNL	Oak Ridge National Laboratory
PSL	polystyrene latex
PT	plasma torch
PWR	pressurized-water reactor
RF	radio frequency
SEM	scanning electron microscope
TEM	transmission electron microscope
TMI	Three Mile Island

AEROSOL RELEASE AND TRANSPORT PROGRAM QUARTERLY PROGRESS REPORT FOR OCTOBER–DECEMBER 1981

R. E. Adams M. L. Tobias

ABSTRACT

This report summarizes progress for the Aerosol Release and Transport Program sponsored by the Nuclear Regulatory Commission's Office of Nuclear Regulatory Research, Division of Accident Evaluation, for the period October–December 1981. Topics discussed include (1) under-sodium tests in the Fuel Aerosol Simulant Test (FAST) Facility, (2) U_3O_8 and Fe_2O_3 in steam (light-water reactor accident) aerosol experiments in the Nuclear Safety Pilot Plant, (3) generation and characterization of cadmium and CdO aerosols in the basic aerosol experimental program, (4) core-melt tests of Zircaloy-clad fuel capsules, (5) initial results of a piston-model bubble oscillation code allowing liquid bypass, and (6) calculations with the UVABUBL code to compare with underwater and under-sodium period measurements in FAST experiments.

---

1. INTRODUCTION

The Aerosol Release and Transport (ART) Program at Oak Ridge National Laboratory (ORNL), sponsored by the Nuclear Regulatory Commission's Office of Nuclear Regulatory Research, Division of Accident Evaluation, is a safety program concerned with aerosol release and transport. The program's scope includes aerosol release from fuel, transport to and release from primary containment boundaries, and behavior within containments. The overall goal of the program is to provide the analytical methods and experimental data necessary to assess the quantity and transient behavior of radioactive aerosols released from reactor cores as a result of postulated events of varying severity up to and including accidents resulting in core melting.

The program is divided into several related experimental and analytical activities as summarized below:

1. studies related to hypothetical liquid-metal fast breeder reactor (LMFBR) core-disruptive accidents (CDAs) that involve fuel interactions, expansion, and thermal behavior within the sodium pool as the resultant fuel-vapor bubble is produced and transported through the sodium to the cover-gas region;
2. development of apparatus to investigate the characteristics and transport behavior of materials vaporized from molten fuel;

3. study of the characteristics and behavior of fuel-simulant aerosols in several small vessels; and
4. production and study of aerosols in the Nuclear Safety Pilot Plant (NSPP) for the validation of models, with particular emphasis on the behavior of mixtures of nuclear aerosol species relevant to both light-water reactor (LWR) and LMFBR systems.

Varying levels of effort are anticipated within these categories, with analytical models accompanying the experimental work. The analytical requirements fall into four categories: (1) fuel response to high rates of energy deposition, (2) fuel-bubble dynamic behavior and transport characteristics under sodium, (3) release of aerosols and associated simulant fission products from heated and melting fuel, and (4) dynamic aerosol behavior at high concentrations in the bubble and containment atmospheres.

An attempt will be made to consolidate and present the analyses and data in a manner that will facilitate direct assessment of the radiological hazard associated with arbitrary hypothetical accident scenarios.

2. EXPERIMENTAL PROGRAM

2.1 Source Term Experiments in FAST/CRI-III

A. L. Wright A. M. Smith
J. M. Rochelle

2.1.1 Introduction

The Fuel Aerosol Simulant Tests (FAST) and the Containment Research Installation-III (CRI-III) tests are performed by using the capacitor discharge vaporization (CDV) technique to place UO_2 fuel samples into the high-energy states that could be produced in LMFBR hypothetical CDAs (HCDAs). The primary goal of the FAST/CRI-III test program is to use the experimental results as a data base for developing analytical models that could be used to predict fuel transport through the coolant in severe accidents.

During the quarter, three under-sodium "shakedown" experiments were successfully performed in the FAST Facility. Test specimen and electrical energy input data are presented in Tables 1 and 2. Individual test results are presented in Sect. 2.1.2.

Table 1. Test specimen data

Test	Pellet stack mass (g)	Pellet stack length (mm)	Microsphere mass (g)	Quartz tube dimension (mm)	
				ID	OD
FAST 101	17.44	90.7	33.92	9.70	17.15
FAST 102	17.33	90.2	35.09	9.70	17.15
FAST 103	17.36	90.4	32.93	9.70	17.15

Table 2. Electrical energy input data[a]

	High preheat power (W)	High preheat resistance (Ω)	CDV time to arcing (ms)	CDV energy input to arcing (ms)
FAST 101	1100	0.94	4.66	38.8
FAST 102	1600	0.48	*b*	*b*
FAST 103	1600	0.43	3.15	37.9

[a]Input capacitor bank energy storage in FAST 101 and 103 ≅ 75 kJ.
[b]FAST 102 was a "preheat-only" test.

2.1.2 Discussion of FAST under-sodium test results

Three under-sodium "shakedown" tests, FAST 101, 102, and 103, were performed this quarter. The goals of these experiments were to (1) demonstrate that the CDV technique can be used to vaporize fuel in a sodium pool; (2) determine the appropriate preheat level to use in the under-sodium tests; and (3) determine if pressure, acoustic, and aerosol measurements can be successfully made in a high-temperature sodium environment.

The results from these tests are discussed in this section. In each test the sodium was heated to a temperature of ~811 K (1000°F), and the pressure of the xenon gas in the test sample was ~0.136 MPa.

2.1.2.1 FAST 101. For this first test, approximately one day was required to move sodium from the dump tanks to the test vessel and to heat the sodium to 811 K. The sodium level above the test sample was set to 0.96 m.

Through experience, the technique of preheating samples in the water tests had been adopted so that the resistance after high preheat would be ~0.5 Ω; a 1700-W high preheat was used to achieve this resistance. In FAST 101, resistance-vs-power data were obtained for low-preheat powers of 400, 500, and 600 W. Extrapolation of this data seemed to indicate that an 1100-W high preheat would lead to a 0.5-Ω final resistance. However, the resistance achieved was 0.94 Ω; this implied that the pellets probably were not molten after preheat.

In spite of this, it was found possible to perform capacitor discharge and vaporize portions of the pellet stack successfully. The CDV energy input time of 4.66 ms was larger than typically achieved in the water tests — most likely due to the cooler sample conditions after preheat. Examination of the condition of the sample holder when it was removed from the test vessel indicated that the sample rupture had occurred.

Pressure measurements were made in the sodium at a distance of 0.23 m from the test sample and in the argon cover gas above the sodium. An oscilloscope trace of the pressure record from FAST 101 is shown in Fig. 1. Although the pressure trace from the transducer mounted near the source is somewhat noisy, the pressure peaks due to bubble collapse and reexpansion can be easily seen. The time between the first two pressure peaks, which is the first bubble oscillation period, was 27.7 ms in this test. It is interesting to note that this is significantly less than the period found in underwater tests — roughly 50 ms — for similar test conditions.

Attempts to sample the argon cover gas were made to determine if UO_2 aerosols were transported through the sodium in this test. The filter paper used in the aerosol sampler was supposed to withstand temperatures of 773 K. However, inspection of the filters after the test seemed to indicate that they had reacted with the sodium vapor because they had turned brown in color and were very brittle. The filters that could be removed from the sampler were sent to analytical chemistry; masses of UO_2 found on the samples were very small and indicated that ~0.5 mg of UO_2 had reached the cover gas. This is roughly 0.003% of the initial pellet stack mass of 17.4 g.

2.1.2.2 FAST 102. Evaluation of results from FAST 101 indicated that the 1100-W high preheat used did not produce pellet melting, and that

ORNL-DWG 82-5274 ETD

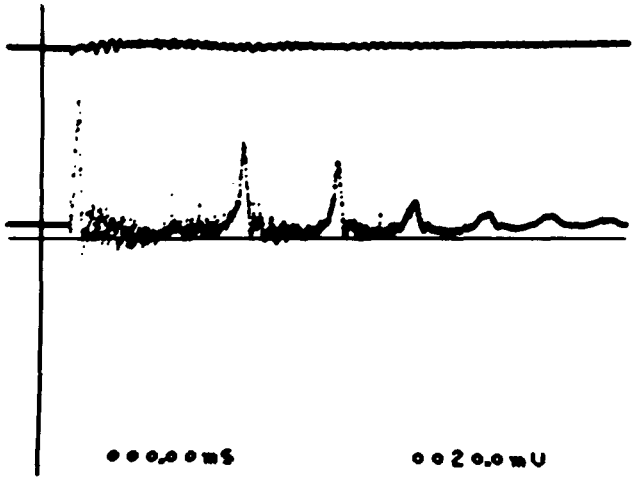

Fig. 1. Oscilloscope trace of pressure vs time measurements from FAST 101. Upper trace is pressure measured in argon cover gas, and lower trace is pressure measured 0.23 m from the test sample. Total time of measurement is ~100 ms.

a 1600-W level would have been more appropriate. FAST 102 was a "preheat-only" under-sodium test using a 1600-W preheat. After the test was completed, the test sample was vacuum impregnated with epoxy resin and sectioned; pictures were then taken of the sample cross section at five locations along its length. Photographic results indicated that about 50% of the pellets became molten; this corresponded well to melt fractions determined photographically from tests done in argon gas. Based on these results, the 1600-W preheat level will be the standard for future under-sodium tests.

A pair of acoustic transducers (transmitter-receiver) was mounted on stainless steel waveguides for this test in order to determine the level of signal that could be transmitted through the sodium. The transmitting transducer was excited with a 10-V_{rms} signal at a frequency of 2.25 MHz. When sodium was first loaded into the vessel, no signal was transmitted through it. A day later, however, a transmitted signal was produced, which suggests that the sodium did not initially wet the vessel wall. The transmitted signal was ~7 mV_{rms}, which corresponds to a total signal attenuation of -63 dB. This was roughly the level of attenuation expected on the basis of fairly simple calculations.

2.1.2.3 FAST 103. For this test the sodium level above the test sample was 1.12 m, the sodium temperature was 811 K, and the cover-gas pressure was 0.122 MPa. Data from this test indicated that the sample energy input at sample rupture was similar to that produced in the underwater tests. Figure 2 illustrates the data obtained from the pressure transducer mounted 0.23 m from the test sample. The initial bubble period of 34.5 ms was somewhat larger than that produced in FAST 101. The short-duration, high-pressure event that occurred at 43.1 ms was not typical of

ORNL–DWG 82–5275 ETD

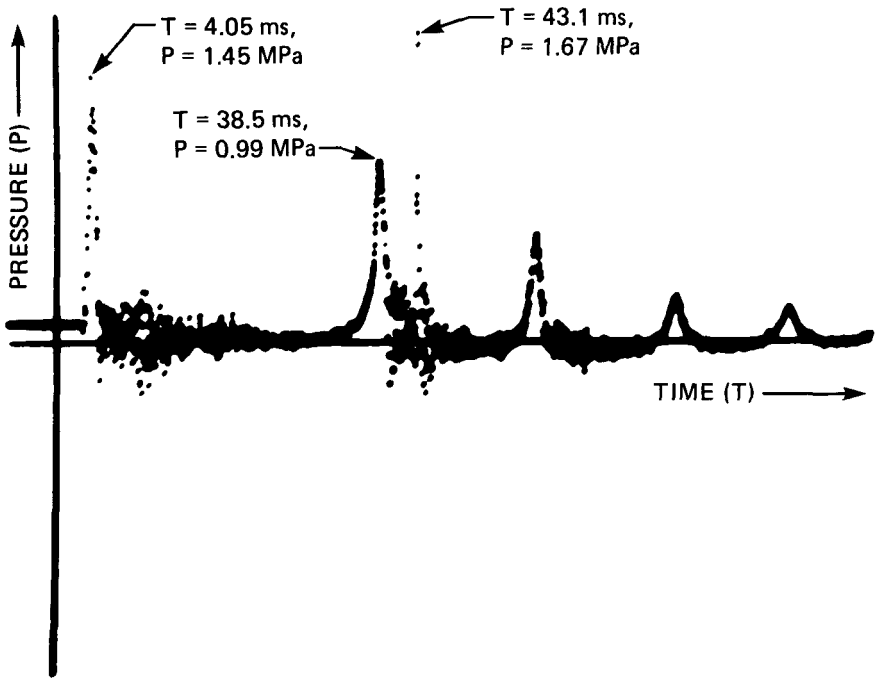

Fig. 2. Picture of oscilloscope trace of pressure vs time from FAST 103. Pressure measured at a distance of 0.23 m from the bubble source.

any event ever observed in the underwater tests. At this point it is possible, but not proved, that this pressure spike may have been the result of a fuel-coolant interaction.

Three pairs of acoustic transducers were mounted on vessel waveguides for this test in an attempt to detect bubble transport. However, the acoustic energy from sample breakup pulsed the RMS meters used to measure transmitted signals, and the meter recovery times of 1 to 2 s did not permit valid measurements to be made.

2.2 Secondary Containment Aerosol Studies in the NSPP

R. E. Adams R. F. Benson
M. T. Hurst

2.2.1 Introduction

Studies relating to the behavior of aerosols released under LWR accident conditions into secondary containment environments were continued. Six single-component aerosol tests involving U_3O_8 aerosol in steam environments and one single-component aerosol test involving Fe_2O_3 aerosol in a steam environment have been conducted. Runs 401–405 have been reported

previously,[1-3] and results from Runs 406 and 501 are contained in this report.

2.2.2 LWR aerosol experiment No. 406

Mixing of the U_3O_8 aerosols within the steam-air atmosphere has not been as uniform as in previous U_3O_8 aerosol tests under dry conditions. During Runs 401-403 (Refs. 1 and 2), an aerosol concentration gradient existed early in each test with the higher concentration existing in the upper portion of the vessel. In an attempt to improve mixing, a small air-driven fan was installed near the bottom of the vessel with the air movement directed upward. Use of this mixing fan during Run 404 (Ref. 3) seemed to enhance the mixing of the aerosol with the steam atmosphere; the fan was operated for about 1 h, measured from start of aerosol generation.

This sixth test in the LWR aerosol study was designed to further observe the influence of forced mixing of the aerosol-steam atmosphere on the aerodynamic behavior of the U_3O_8 aerosol. This test duplicated Run 404 in most details except that the fan-mixer was operated for the first 9.5 h of the test rather than for 1 h as in Run 404.

As in previous tests, steam was introduced into the closed NSPP vessel, which was at 0.039 MPa, to bring the vessel atmosphere to an average temperature of 374 K and a pressure of 0.164 MPa. This process required about 1 h. At this point the rate of steam injection was reduced, and the accumulated steam condensate, which had collected in the vessel during heat-up, was removed to a holding tank. The U_3O_8 aerosol generation was then started, and the introduction of the aerosol into this environment continued for 9 min. Steam injection at the lowered rates continued for a period of 6 h. During this period the pressure and temperature slowly increased to about 0.195 MPa and 382 K, respectively. The vessel and its contents were allowed to cool for about 18 h after termination of the low-level steam injection.

During the test, measurements were made of aerosol mass concentration, particle size, fallout and plateout rates, total fallout and plateout, vessel atmosphere temperature, temperature gradient near the vessel wall, pressure, moisture content, and steam condensation rate on the vessel wall.

2.2.2.1 Aerosol mass concentration. The maximum average U_3O_8 aerosol mass concentration was about 15.2 $\mu g/cm^3$, which is comparable with the 23 $\mu g/cm^3$ aerosol concentration achieved during Run 404. Operation of the fan-mixer during Run 406 improved the mixing of the steam and aerosol considerably as compared to that observed during the early phases of Run 404. Figure 3 contains the results from seven aerosol mass samplers. Samplers 151 and 152 are located in the upper region of the vessel; sampler 153 is located about midplane of the vessel; and sampler 154 is located in the lower region of the vessel. Samplers 155-157 penetrate the vessel wall at about the same elevation as sampler 153.

The influence that operation of the fan-mixer had on aerosol behavior may be observed by comparing the results of Runs 404 and 406 with those of Run 403 where the fan-mixer was not used. Figure 4, which compares these three runs on the basis of a normalized aerosol mass concentration, shows

ORNL–DWG 82–5276 ETD

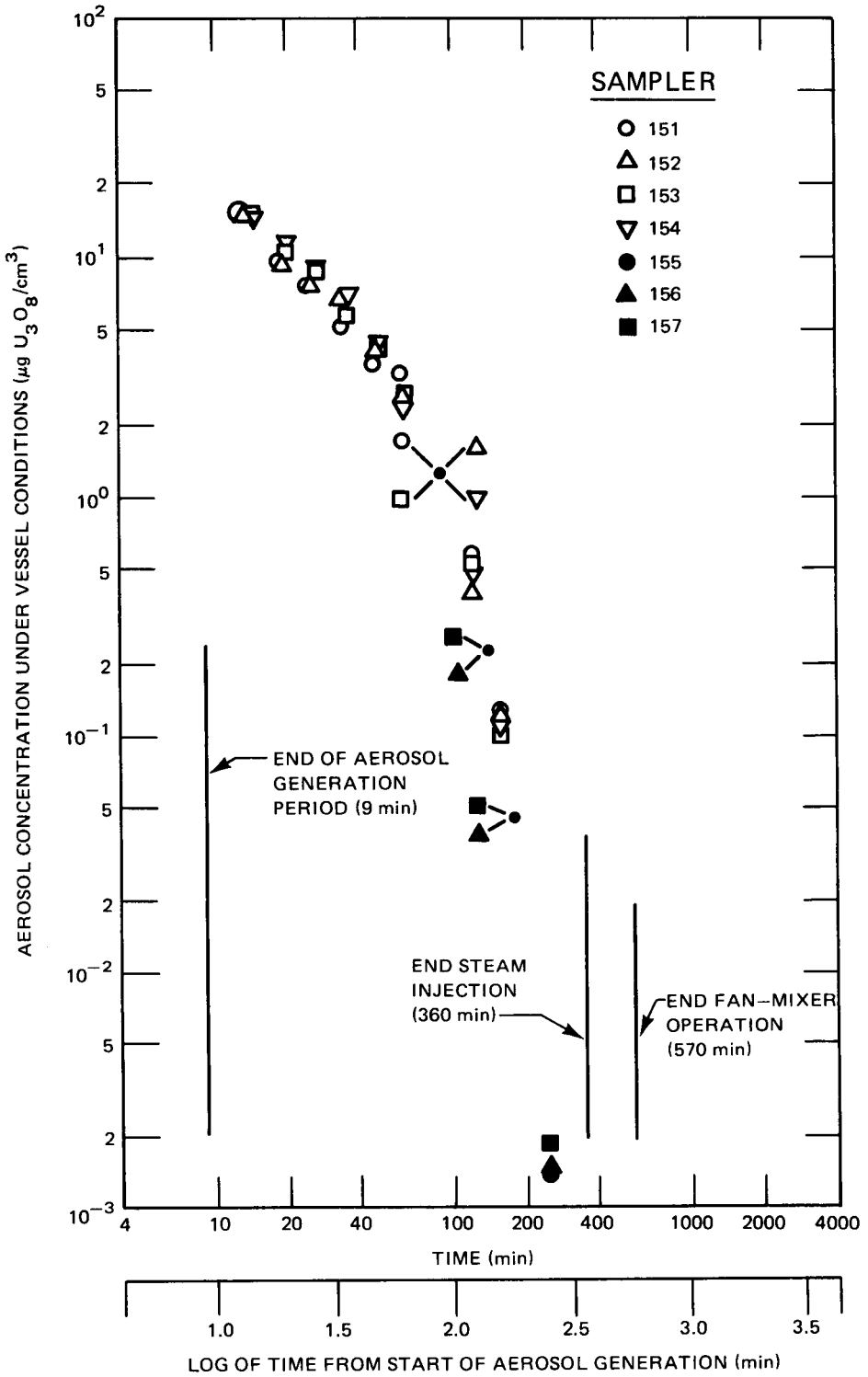

Fig. 3. U_3O_8 aerosol mass concentration as a function of time for Run 406. Note that aerosol concentration is calculated under temperature and pressure that existed in vessel at time of sampling.

ORNL–DWG 82–5277 ETD

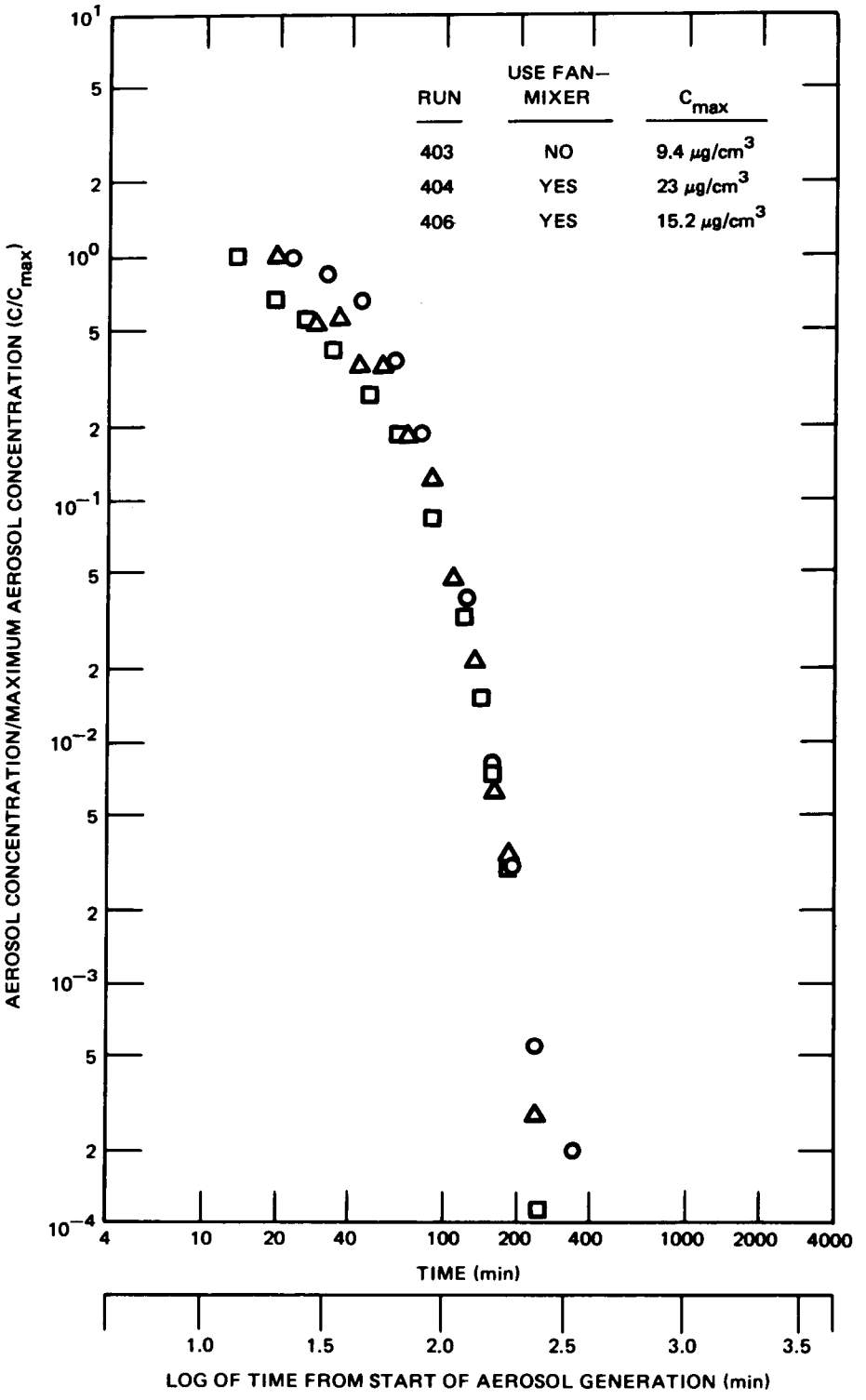

Fig. 4. Comparison of behavior of U_3O_8 aerosol in Runs 403, 404, and 406. Use of fan-mixer in Runs 404 and 406 may have caused early reduction in aerosol mass concentration.

that during the first hour or so, there is an accelerated rate of removal of the aerosol mass from the vessel environment when the fan-mixer is used. This air movement may be responsible for an increase in aerosol particle size through turbulent agglomeration, causing enhanced aerosol fallout or impaction on surfaces within the vessel. This behavior of the aerosol in Runs 404 and 406 was also reflected in increased aerosol fallout and plateout over the first hour of the experiments.

Although there appears to be an initial loss of aerosol through use of the fan-mixer, the rate of disappearance of aerosol after about 1.5 h is the same for all three experiments. Duration of fan-mixer operation is not a factor after the initial 1.5 h-period.

2.2.2.2 Aerosol particle size. The aerodynamic mass median diameter (AMMD) of the U_3O_8 aerosol was measured both by impactor and centrifuge samplers. The "wet" aerosol was dried by dilution with dry air prior to introduction into the samplers. The AMMD of the "dried" aerosol ranged from about 1.5 to 2 μm over the first 1.5 h of the run. These values are comparable with those measured in the previous steam tests.

2.2.2.3 Aerosol distribution. At the termination of the test (24 h), the approximate aerosol distribution, as determined by both the total fallout and plateout samplers and the final filter sample, was as follows: aerosol settled onto the floor of the vessel, 74%; aerosol plated onto internal surfaces, 26%; and aerosol still suspended in the vessel atmosphere, nil.

2.2.3 LWR aerosol experiment No. 501

The purpose of this test was to observe the influence of condensing steam on an aerosol composed of Fe_2O_3 particles. This is the first in a series of tests using Fe_2O_3 as a simulant for aerosols emanating from molten core support and structure materials. The aerosol was produced by introducing iron powder and oxygen gas into the plasma torch generator, which was installed in the top of the vessel. Operational procedures were the same as utilized in the U_3O_8 aerosol tests. Steam was introduced into the closed NSPP vessel, which was at 0.041 MPa (absolute), to bring the vessel atmosphere (air) to an average temperature of 382 K and a pressure of 0.201 MPa (absolute). This procedure required almost 1 h. At this point, the rate of steam injection was reduced, and the accumulated steam condensate, which had collected in the vessel during heat-up, was removed to a holding tank. The Fe_2O_3 aerosol generation was then started, and introduction into the steam environment continued for 14 min. Steam injection at low rates continued for a period of 6 h. During this period, the pressure and temperature increased to 0.250 MPa (absolute) and 390 K at 2.8 h; at termination of steam injection the values were 0.239 MPa and 389 K. Vessel cooldown continued for the next 18 h. Sampling procedures and parameters were the same as used in Run 406.

2.2.3.1 Aerosol mass concentration. The maximum average Fe_2O_3 aerosol mass concentration was 0.91 μg/cm³ at 4.6 min after termination of aerosol generation. Operation of the fan-mixer produced a fairly homogeneous mixture of aerosol and steam as evidenced by Fig. 5, which contains the results from the seven individual aerosol mass samplers.

ORNL–DWG 82–5278 ETD

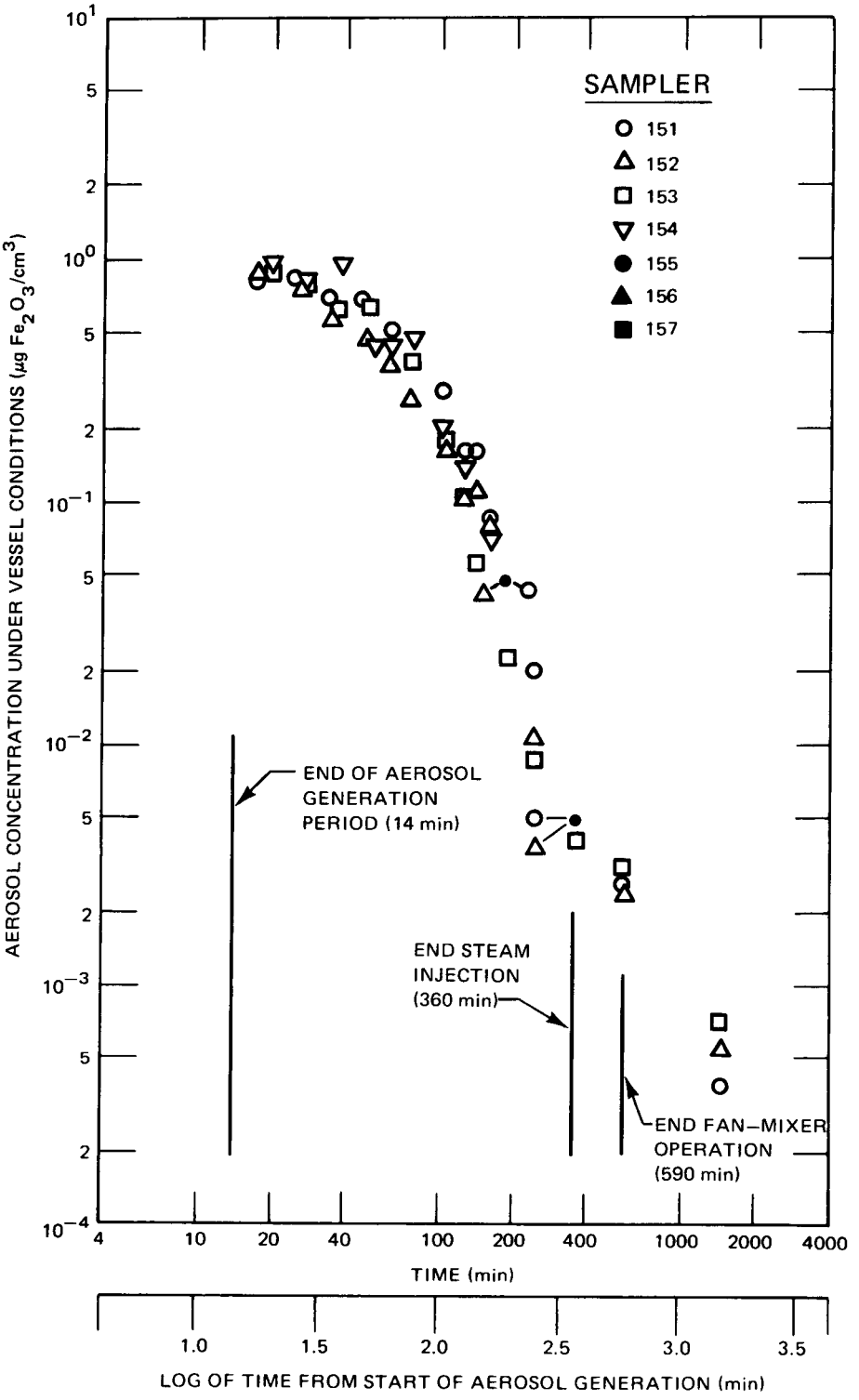

Fig. 5. Fe_2O_3 aerosol mass concentration as a function of time for Run 501. Note that aerosol concentration is calculated under temperature and pressure that existed in vessel at time of sampling.

As already noted in the U_3O_8 aerosol tests, the behavior of the steam strongly influenced the aerodynamic behavior of the test aerosol; this same behavior is observed in the Fe_2O_3 aerosol test. On the whole, there is a small difference in behavior between the U_3O_8 and Fe_2O_3 aerosols. This difference in behavior may be caused by a difference in aerosol concentrations; no U_3O_8 aerosol tests in steam were conducted in the 1 $\mu g/cm^3$ concentration range. The next Fe_2O_3 aerosol test is intended to be in a higher concentration range; data from this run will allow a better comparison to be made of the behavior of these two aerosols.

2.2.3.2 Aerosol particle size. The AMMD of the Fe_2O_3 aerosol was measured both by the impactor and the centrifuge sampler. The "wet" aerosol was dried by dilution with dry air, as before. The AMMD of the "dried" Fe_2O_3 aerosol ranged from 1.0 to 1.6 μm over the first 3.4 h of the test. Scanning electron microscope (SEM) pictures of the "dried" Fe_2O_3 aerosol show spherical clumps of aerosol particles quite similar in appearance to "dried" U_3O_8 aerosol. The most notable difference is in the size of the primary particles; those of the Fe_2O_3 aerosol are much smaller than those of the U_3O_8 aerosol.

2.2.3.3 Aerosol distribution. At the termination of the test (24 h), the approximate aerosol distribution, as determined by both the total fallout and plateout samplers and the final filter samples, was as follows: aerosol settled onto the floor of the vessel, 94%; aerosol plated onto the internal surfaces, 6%; and aerosol still suspended in the vessel atmosphere, nil.

2.3 Basic Aerosol Experiments in CRI-II

G. W. Parker G. E. Creek
A. L. Sutton, Jr.

2.3.1 Introduction

This program of basic experiments is carried out in the 5-m^3 test vessel, CRI-II, as part of the ART Program. Vapor-condensation aerosols likely to comprise mixtures of importance in various nuclear accidents are systematically produced in 100-g quantities and then characterized. Generation techniques until recently were based on powdered metal-oxygen combustion in a dc plasma arc or, in the case of sodium, by ignition of the liquid metal in a high-pressure spray. These processes, of course, produced only the oxide forms. Recently, due to the current interest in a limited number of pure metallic aerosols the plasma torch has been adapted to produce vapor-condensation aerosols of the more volatile metals without oxidation.

In the program of basic aerosol experiments, there will be continuing investigations of the fundamental properties of the single-component aerosols including those of tin, silver, cadmium, and indium for the pressurized-water reactor (PWR); tin and boron for the boiling-water reactor (BWR); and calcium, aluminum, and silicon for the concrete basemat interaction products for core meltdown.

A simplified summary of the systematics of size distribution and deposition rate of as many of these aerosols as possible should be a practical result of these experiments.

2.3.2 Characterization of the aerosols of cadmium metal and CdO

Experiments conducted recently in the parallel program to characterize core-melt aerosols have served to indicate the important contribution to the total aerosol mass of the PWR control rod alloy metals, silver, cadmium, and indium and of the tin component of the Zircaloy fuel cladding in both types of LWRs. Since cadmium appears to be the most volatile component of PWR control rods it was selected initially for characterization of its aerosol forms. Cadmium oxide was inadvertently generated first because the argon-4% hydrogen gas mixture in the containment vessel, due to an unexpected inleakage of air during filling, contained enough oxygen to ignite the cadmium metal vapor and produce a dense crystalline orange-yellow oxide of a somewhat unusually high aerodynamic particle diameter and a very low value for the geometric standard deviation. The AMMD values are listed in Table 3 and may be compared with those of various other noncrystalline aerosols produced with stoichiometric oxygen in the plasma torch. The appearance of the crystalline primary particles in a chain agglomerate is shown in Fig. 6.

Cadmium metal was first successfully vaporized in a dark metallic form after carefully eliminating oxygen from the containment atmosphere with extensive leakage corrections and resorting to operating at positive pressure. Removal of traces of oxygen in a slightly pressurized hydrogen-argon atmosphere was accomplished by operating the dc plasma torch for

ORNL-PHOTO 6029-82

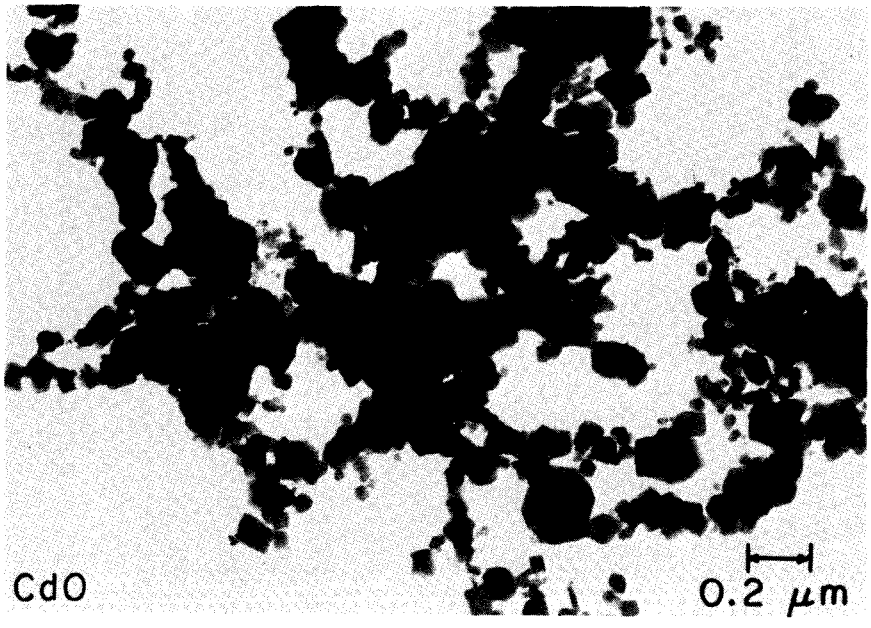

Fig. 6. CdO aerosol agglomerate showing crystalline particles.

Table 3. Size and composition of chain agglomerate aerosols

Aerosol source (Run No.)	Aerosol form (x-ray)	Measured BET surface (m^2/g)	Diameter of average primary (μm)	Primary particles per agglomerate (number)	Maximum airborne concentration (g/m^3)	Agglomerate[a] AMMD (μm)
CDV 16[b]	UO_2	13.0	0.04	1.4×10^4	2.8	1.0
AF 8[c]	UO_2	3.0	0.16	400	6.0	1.6
PT 20[d]	U_3O_8	7.2	0.11	2.0×10^3	50.0	6.0
PT 44	Fe_2O_3	25.0	0.05	4.0×10^4	5.0	3.7
PT 45	SnO_2	7.3	0.12	1.5×10^3	20.0	4.4
PT 47	SiO_2	38.0	0.07	9.0×10^4	7.5	3.1
PT 50	B_2O_3	36.2	0.09	1.6×10^4	7.3	3.3
PT 51	Al_2O_3	28.3	0.05	1.1×10^5	18.0	3.4
PT 52	Al_2SiO_5	18.4	0.09	2.0×10^4	30.0	3.5
PT 53	CdO	6.6	0.11	5.3×10^3	8.0	6.1
PT 54	Cd (metal)	2.5	0.27	200	9.0	8.6

[a]Size from spiral centrifuge data.

[b]CDV = capacitor discharge vaporizer.

[c]AF = arc furnace.

[d]PT = plasma torch.

several minutes without metal feed and thus allowing the hot hydrogen to deplete the oxygen. Metal feeding was then introduced while the containment gas pressure was several pounds gage positive. This resulted in a pure metallic aerosol with an even greater aerodynamic mass median diameter than the corresponding oxide and a very narrow size distribution. The primary particles as seen in an electron photomicrograph are shown in Fig. 7. The rates of change in airborne mass concentration for cadmium and CdO are shown in Fig. 8. The distinct difference in the two curves suggests corresponding differences in the size and nature of the aerosol agglomerates, as is confirmed by the values in Table 3.

Particle size distributions for CdO and cadmium metal as determined with the spiral centrifuge are shown also for comparison in Fig. 9 in the form of fraction in a size increment vs the width of the increment. The distribution data are also shown for comparison by the log-probability graphic method in Fig. 10.

In this program, metallic silver and metallic tin should be the next in order for characterization.

2.4 Core-Melt Aerosol Release and Transport

G. W. Parker G. E. Creek
A. L. Sutton, Jr.

2.4.1 Introduction

The core-melt ART experiments are intended to address phenomena associated with LWR Class IX accidents, particularly the postulated large-scale vaporization of fission products, core components, and structural materials. To attain the desired high temperatures and melting rates, the rf induction melting of Zircaloy-clad fuel pins in presintered powdered oxide shells of UO_2 or ZrO_2, the "skull-melting" technique, has been chosen as the basis of the experimental system. A wide variety of core-simulating charge mixtures may be used in this method, and fission product tracers may also be employed. Additionally, apparatus scale-up appears to be reasonably straightforward.

2.4.2 Observations on the silver alloy control rod interaction with fuel cladding

For the average operating PWR approximately 2300 kg of silver alloy is used in the form of full-length stainless steel clad rods inserted into the core of the reactor through approximately 16 guide tubes for each assembly. That this quantity of relatively low-melting metal should have significant effect upon accident analysis became known after the Three Mile Island (TMI) incident and has thus become an integral part of the present core-melt aerosol study.

In order to provide a representative alloy for the core-melt experiments, a midlife mixture, which has the composition shown in Table 4, was selected from the Reactor Handbook.[4] These values result from neutron capture in a beginning composition of 80% Ag, 15% In, and 5% Cd.

ORNL–PHOTO 6030–82

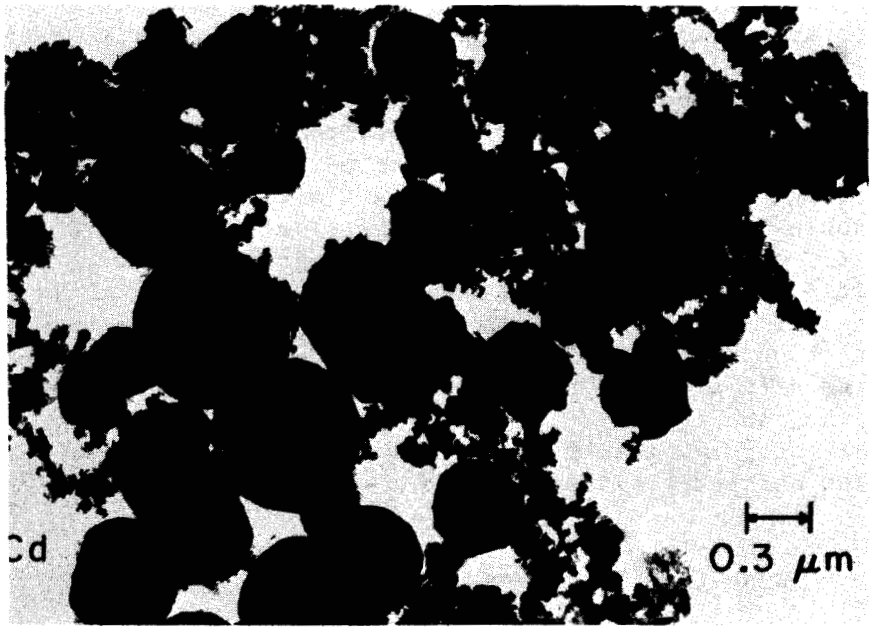

Fig. 7. Cadmium metal aerosol agglomerate showing mainly spherical particles.

ORNL–DWG 82–175A

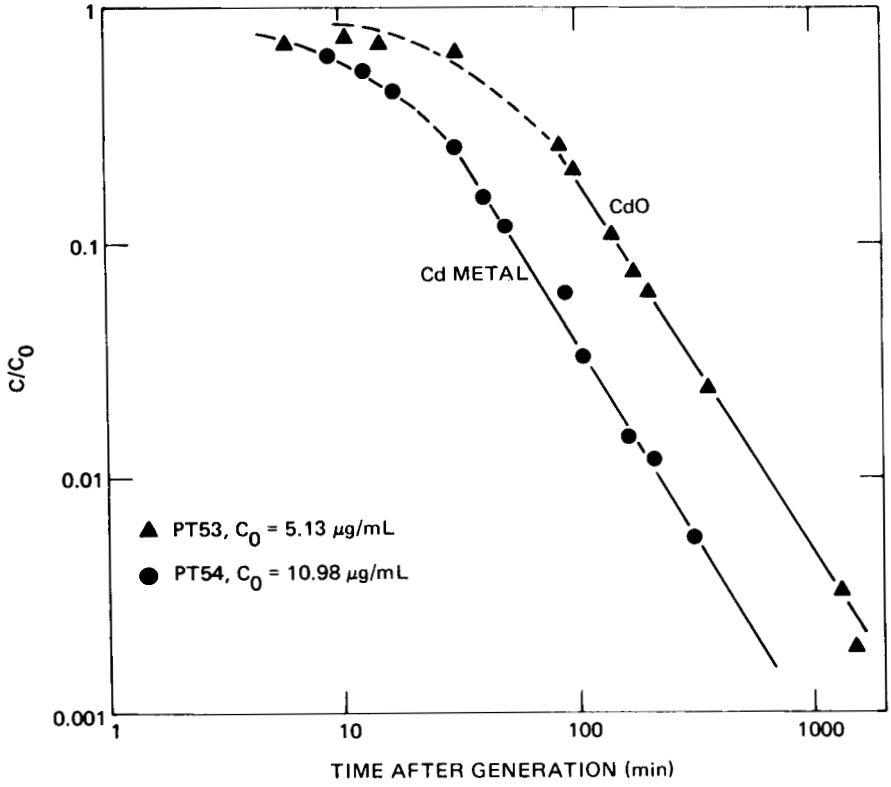

Fig. 8. Relative rate of change in airborne mass concentration for cadmium and CdO.

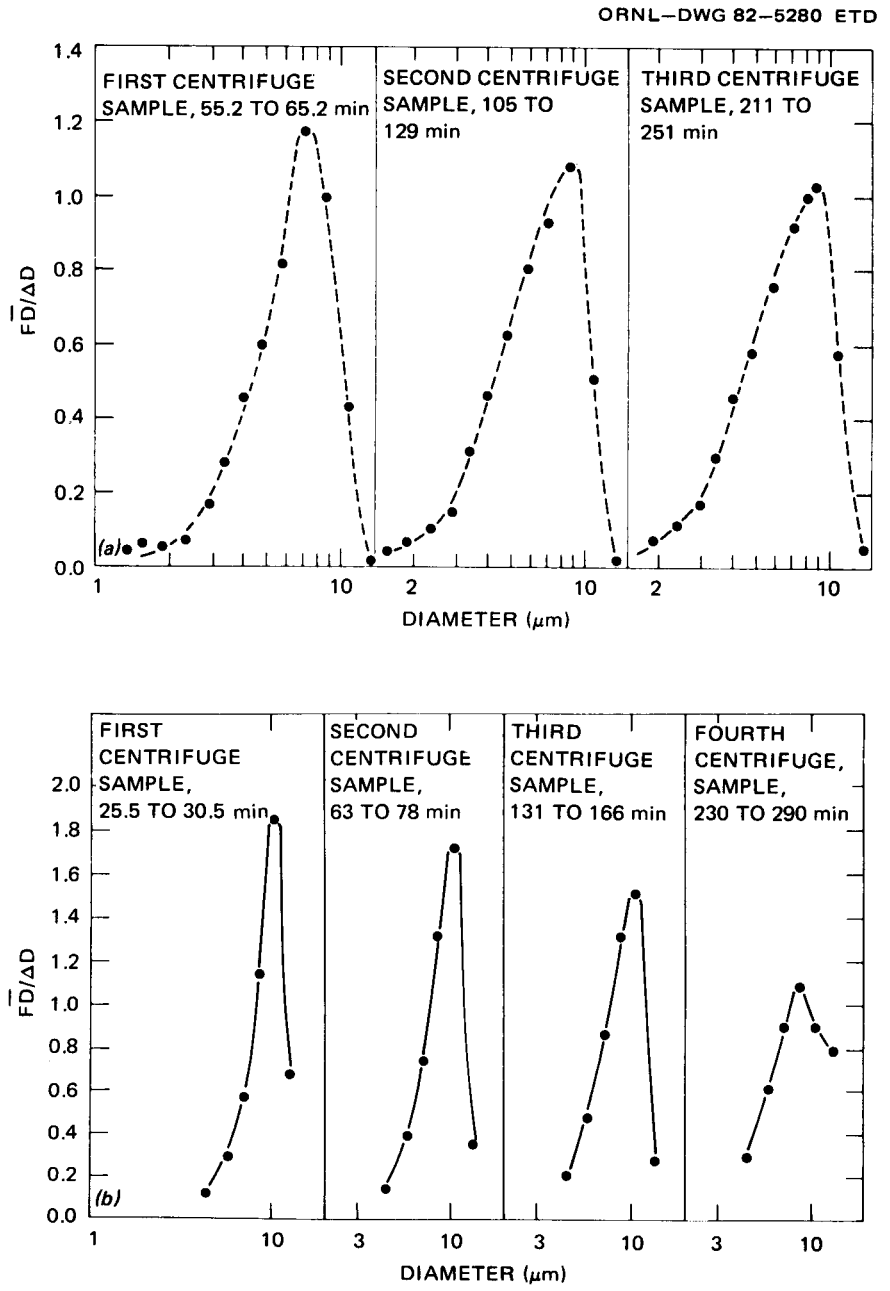

Fig. 9. Fractional size distribution of aerosols of (a) CdO (PT53) and (b) cadmium metal (PT54) showing rate of change more pronounced in cadmium metal.

ORNL–DWG 82–5281 ETD

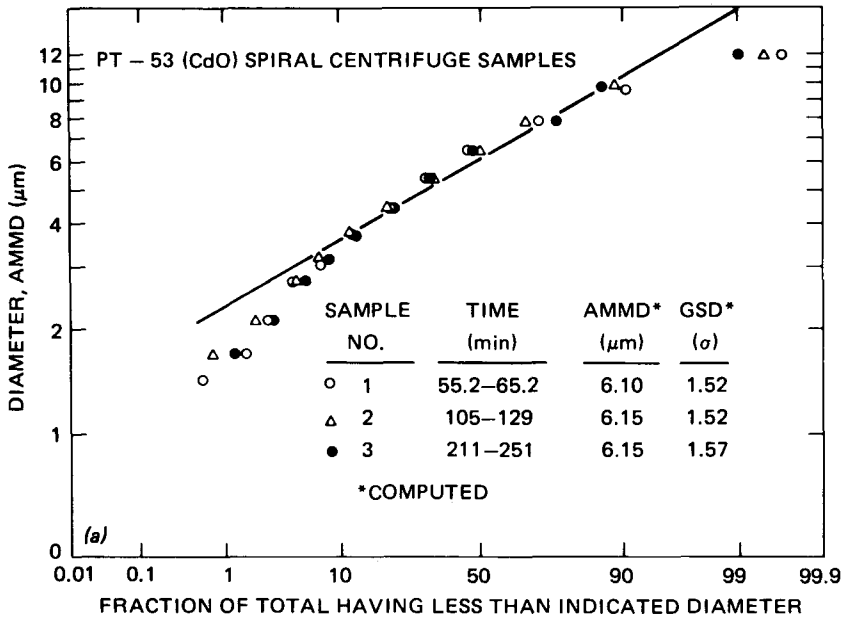

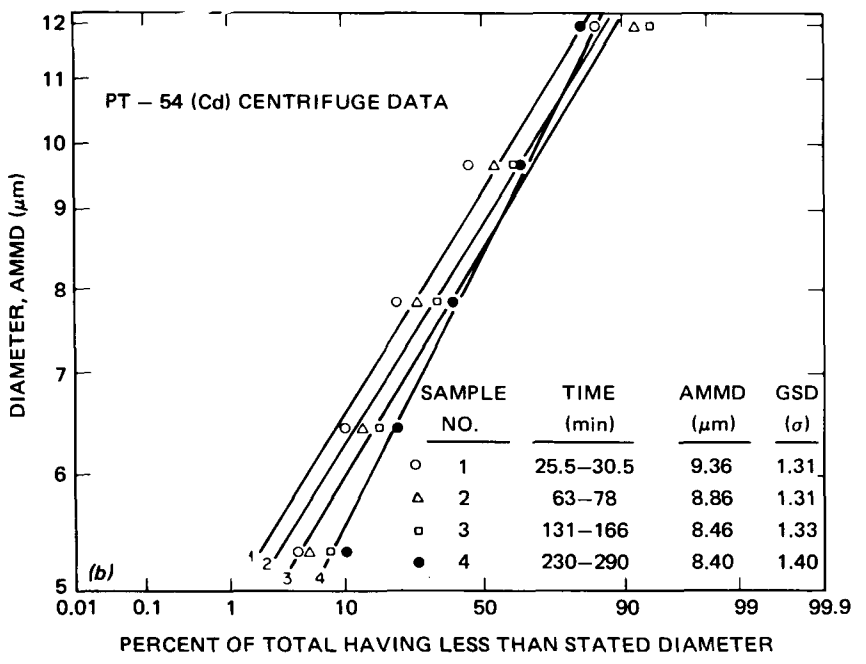

Fig. 10. (a) CdO and (b) cadmium metal aerosol AMMD and size deviation for Runs PT53 and PT54.

Table 4. Control rod alloy 2567

Element	Weight (%)
Ag	76.3
In	12.1
Cd	9.4
Sn	2.0

The mass ratio of silver alloy to Zircaloy in a PWR varies with vendors between 10 (Ref. 5) and 17% (Ref. 6). For our studies we have uniformly used the lower value. Implications of the effect of the range of values should not be overlooked.

Several experiments have been conducted to illustrate the initiation of a candling-type of clad melt-silver alloy interaction, which was first observed by S. Hagen and reproduced photographically in 1978 in the progress report KFK 2750 (Ref 7). According to Hagen the stainless steel tube containing the silver alloy control rod burst when heated to 1400°C as a result of the internal vapor pressure exerted by the cadmium component, and the molten alloy extensively covered parts of the zircaloy cladding throughout the fuel bundle. Then upon heating the bundle to 1700°C a low-melting silver-zirconium alloy was melted off of the free standing fuel and then refroze at the base of the fuel bundle.

Both of Hagen's observations have been confirmed here in separate tests. In one of these, a section of stainless steel tubing containing a full-size control rod was seal welded in helium and placed in a resistance furnace, where it was heated in successive steps to 1350°C. After this time when no swelling was noticed, the specimen was heated to 1405°C at which temperature it burst by complete weld failure at one end. The appearance of the specimen shown in Fig. 11 essentially confirms the 1400°C value in Hagen's report.

In core-melt Test 14, a bundle of 12 Zircaloy-clad fuel capsules about 10 cm long were mounted at reactor spacing with two stainless steel spacer plates. The configuration is shown in Fig. 12(a). The loading details are shown in Table 5.

The assembly was heated slowly in steam over a period of 7.5 min to a maximum temperature of about 1800°C (estimate). Examination revealed the free standing fuel as shown in Fig. 12(b) with essentially all of the metallic components "candled" to form a solid base that showed evidence of interaction with the ZrO_2 crucible.

An analysis of the yield of both the aerosols carried to the downstream filter by the hydrogen and that plated out in the furnace chimney showed that it consisted of about 6.5% of the cadmium and 0.35% of the silver. No other constituent was detected.

ORNL-PHOTO 6031-82

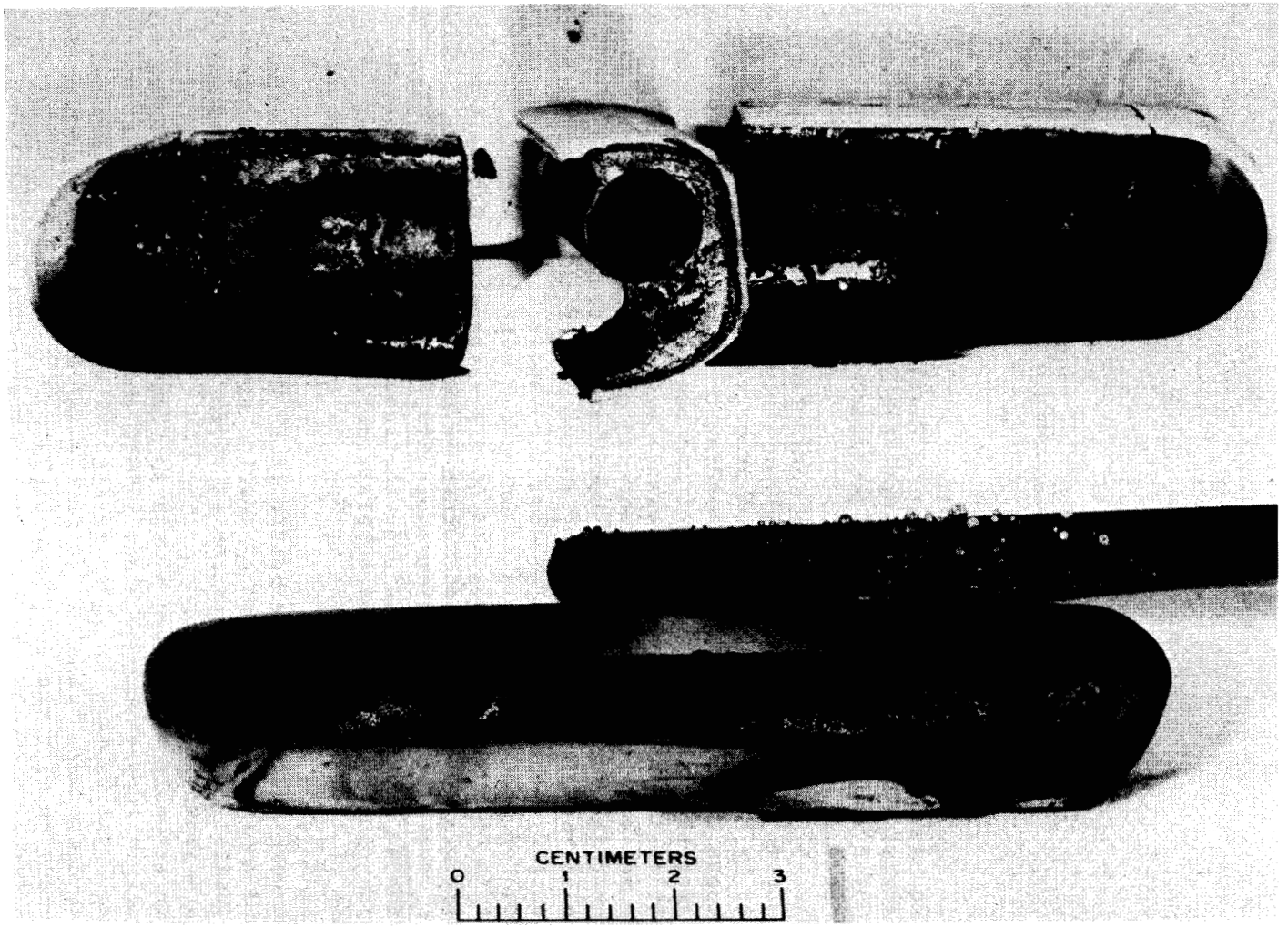

Fig. 11. Test specimens used to confirm the failure of the control rod tube (below) and the silver-Zircaloy interaction (above).

ORNL–PHOTO 6032–82

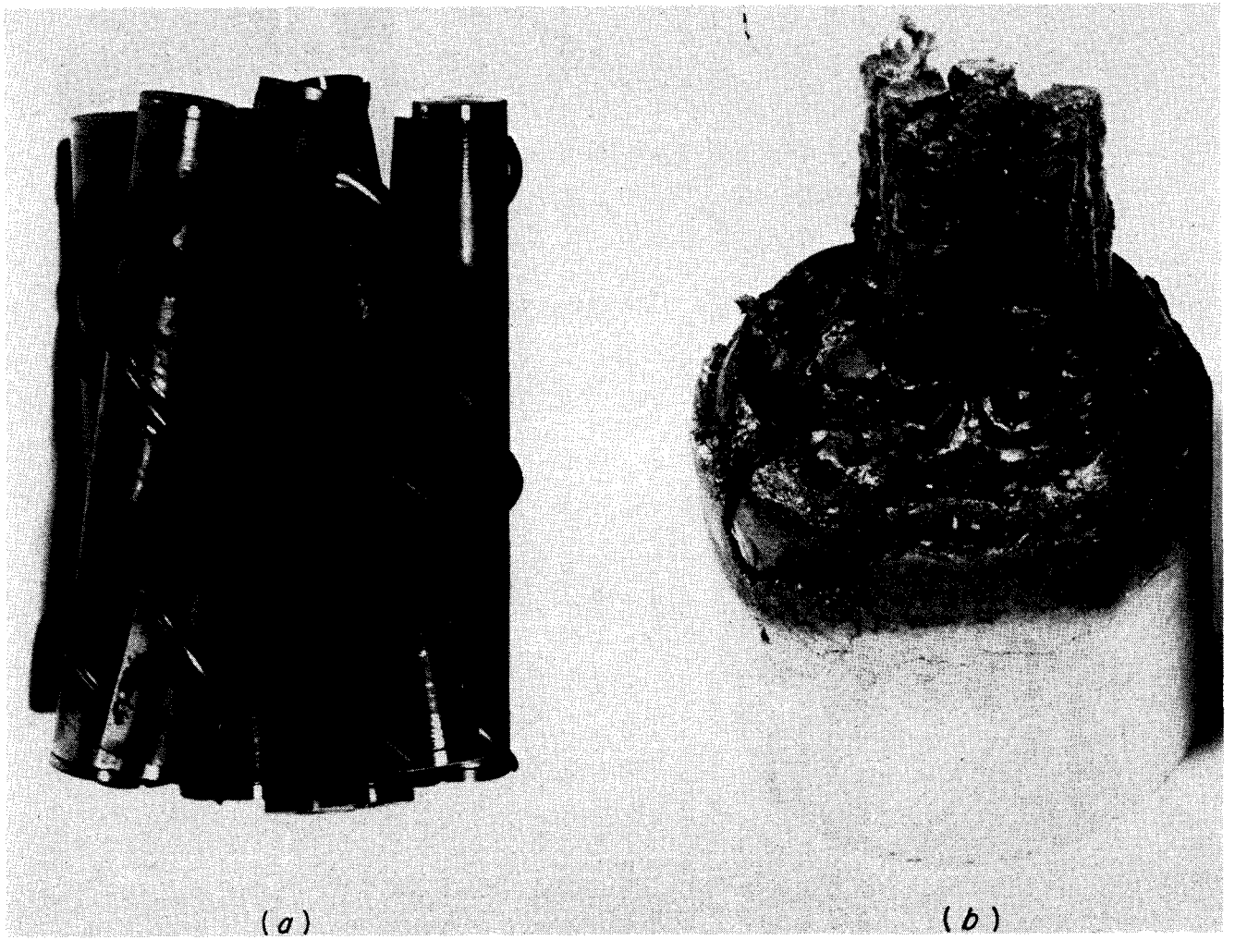

Fig. 12. Steps in the silver-Zircaloy candling process at 1400°C (a) showing Zircaloy wetted by the silver alloy and cladding completely melted off and (b) at 1800°C.

Table 5. Core-melt Test 14

UO_2	712 g
Zry-4	178 g
SS	49.5 g
Ag, In, Cd	10.5 g (Rod in SS tube)
H_2O added	27 mL
H_2 released	22 L (equal to 25% Zr oxidation)

An extended core-melt experiment, Run 16, was next conducted in which the following loading (Table 6) in a fuel bundle was subjected to three incremental increases in temperature, and the residue after melting is pictured in Fig. 13.

The aerosol release data were determined for approximately equal intervals of heating time to 1800, 2200, and 2400°C. The relative composition of the aerosol collected on the downstream filter was first determined by direct x-ray fluorescence analyses as illustrated in Fig. 14. The prominence of cadmium in the first heating and of the silver at the higher temperatures was evident in the filter sample (Table 7) as well as in the furnace plateout (Table 8). The mass was divided about equally between the two fractions.

A summary of the total volatile material released is given in Table 9. In this case over half of the cadmium (53%) was released and about the same mass of silver (but only 6.1% of the inventory). About 5.4% of the indium was released. Almost no tin (0.2%, which includes the inventory of tin in the Zircaloy) was released. There was also a trace of uranium (1×10^{-3}%) released, mainly on to the furnace wall.

Table 6. Core-melt Test 16

UO_2	481 g
Zry-4	156 g
Ag, Cd, In	10.6 g
H_2O added	53 mL
H_2 released	58 L (76% Zr oxidation)
Total time heated	14.5 min to 2400°C

ORNL–PHOTO 0749–82

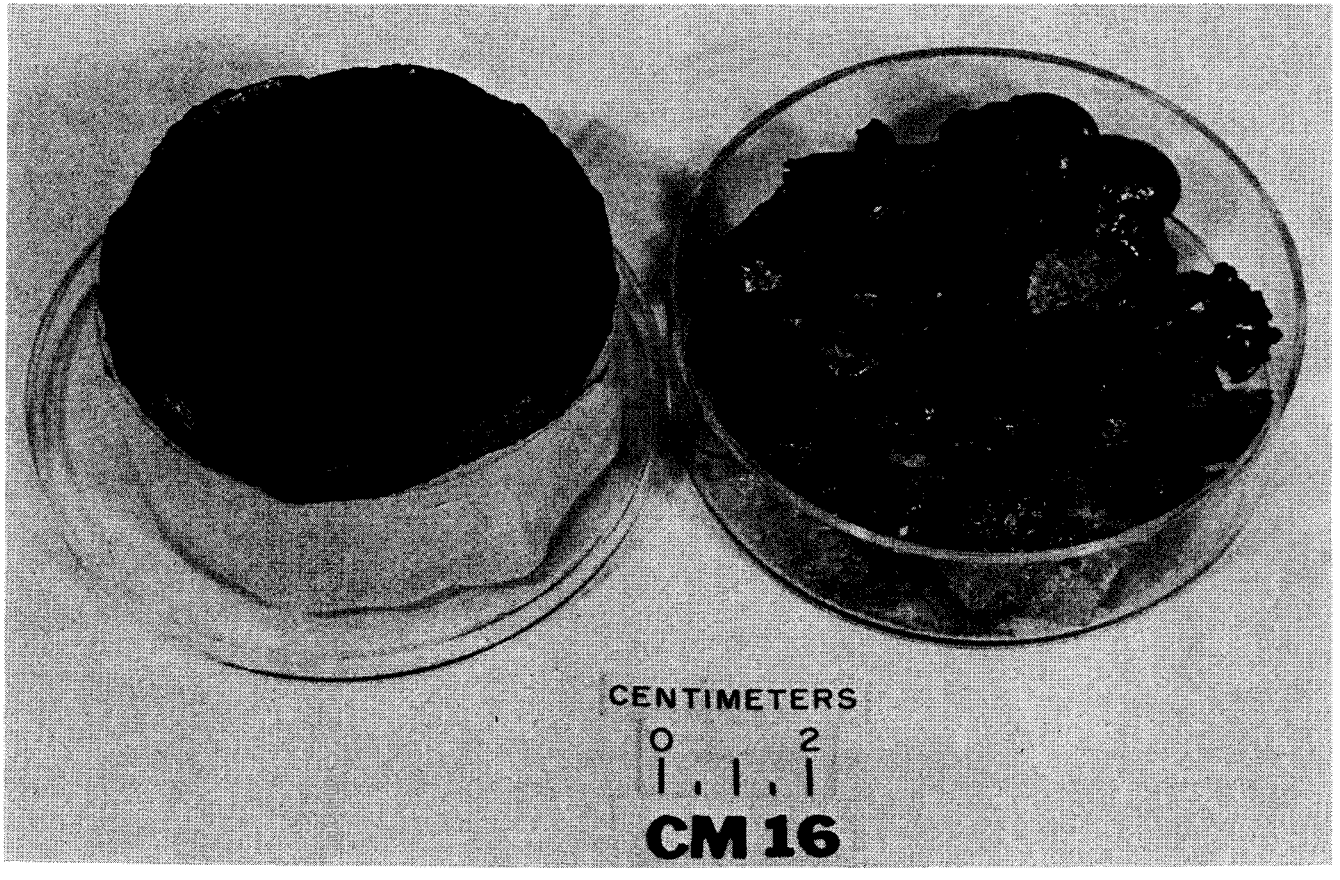

Fig. 13. Core-melt residue from Test CM-16 after heating to 2400°C.

ORNL–PHOTO 6033–82

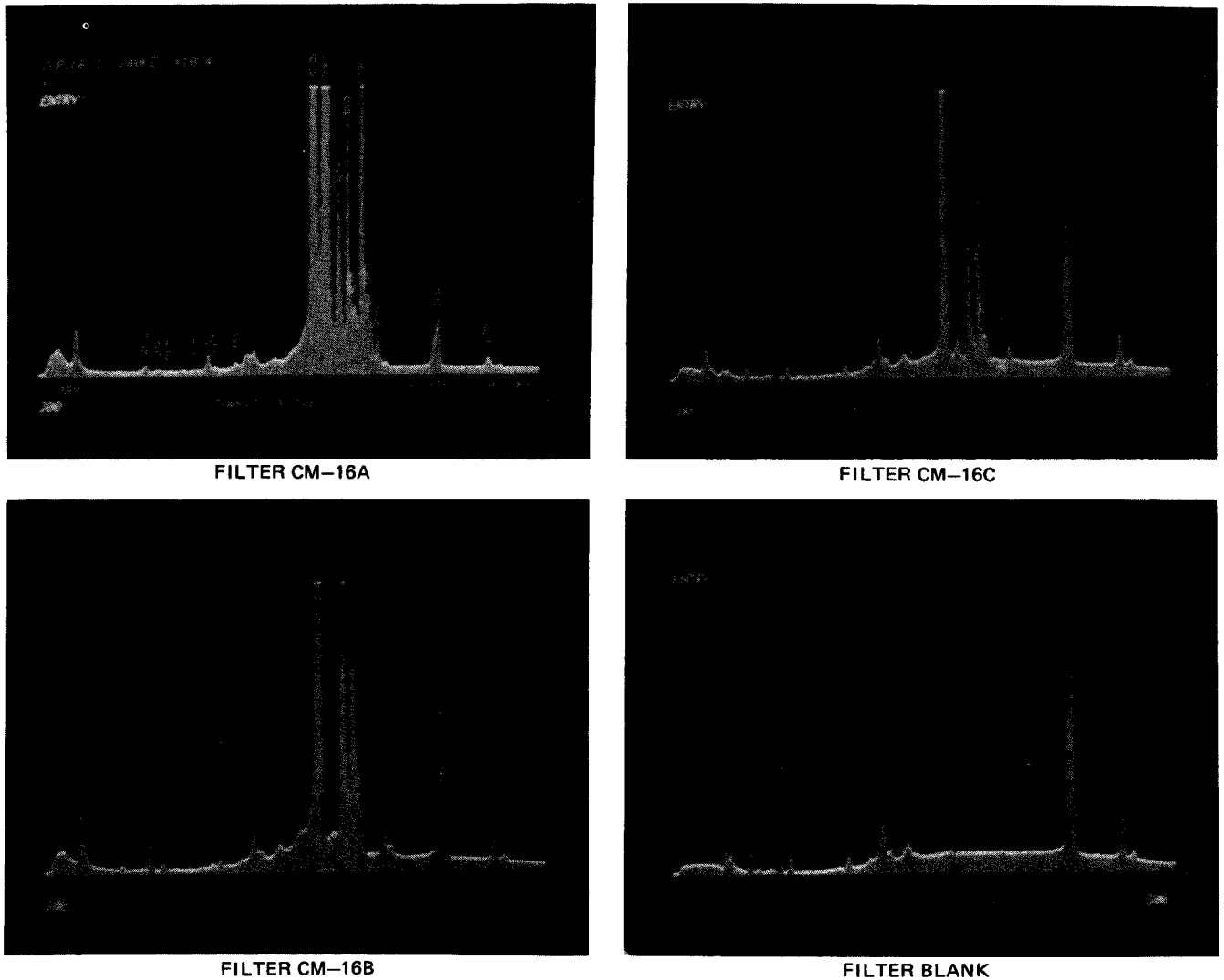

Fig. 14. X-ray fluorescence analyses (EDAX) of silver alloy metals vaporized in core-melt Experiment 16.

Table 7. CM-16 filter paper analyses

Sample No.	Maximum temperature (°C)	Release (mg)	Analysis (wt. in mg)				
			Cd	Ag	In	Sn	U
16-A	1800	294	178	103	9	3	<1
16-B	2200	103	1	80	20	1	<1
16-C	2400	23	<1	17	3	<1	<1

Table 8. CM-16 furnace deposited aerosols

Sample No.	Maximum temperature (°C)	Release (mg)	Analysis (wt. in mg)				
			Cd	Ag	In	Sn	U
16-A	1800	345	270	73	<1	<1	
16-B	2200	175	<1	158	15	<1	
16-C	2400	218	83	108	21		6

Table 9. CM-16 total aerosol release

Element	Mass released (g)	Percent of mass inventory
Cd	0.53	53
Ag	0.54	6.1
In	0.07	5.4
Sn	0.005	0.2
U	0.006	1×10^{-3}

From this experiment it is obvious that the control rod alloy dominates the aerosol formation for the PWR core meltdown. A decidedly different aerosol should be expected when a BWR-type assembly is subjected to a similar meltdown. (The control rods there are based on boron carbide and do not contain silver.)

3. ANALYTICAL PROGRAM

3.1 Modeling Bubble Oscillation Including Effects of Inertia of the Surrounding Fluid

M. L. Tobias

3.1.1 Introduction

The "piston" oscillation code described in the previous quarterly report[3] has been extended to include the inertial effects of fluid motion around the bubble. There were two purposes for this study. The first was to determine if there were any changes in the bubble oscillation pattern due to such flow; the second was to examine the effects of such motion as a function of bubble depth.

The model was constructed using both the PV^{γ} = const. as the equation for adiabatic gas motion and with the use of the actual properties of a saturated liquid-gas mixture of UO_2. The equations derived are based on the layout of the physical situation shown in Fig. 15(b), an idealization of the spherical bubble expansion situation shown in Fig. 15(a). The bubble is assumed to be a cylindrical volume of fixed cross-sectional area A held between upper and lower liquid regions. These are connected by a pipe of fixed length of cross section AP through which liquid can flow in either direction. The bubble is assumed to expand adiabatically. For numerical checking purposes, liquid motions are assumed frictionless, although this is not a necessary restriction.

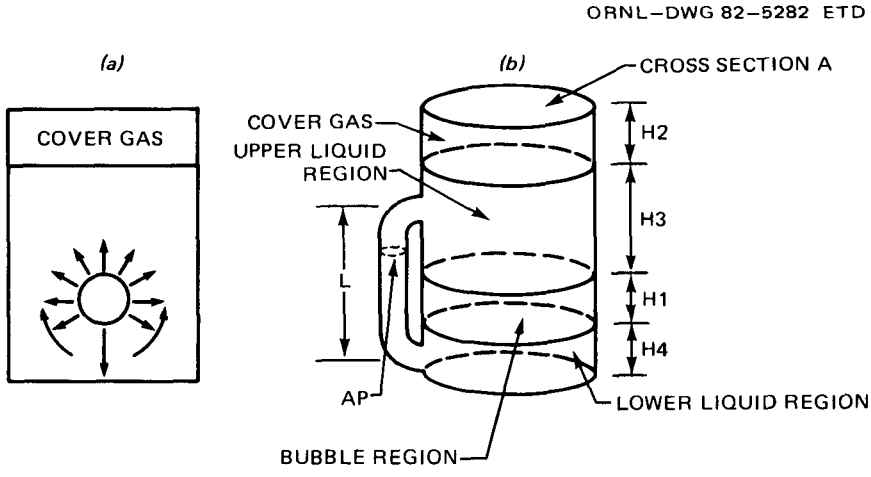

Fig. 15. (a) Expanding bubble in FAST experiment causes fluid motion and (b) idealization of the expanding bubble as a cylindrical region.

3.1.2 Differential equations of the system

The computer code was constructed on the basis of three simultaneous differential equations, one for each region. Each is derived on the basis of conservation of momentum.

Lower Liquid Region:

$$d^2(H4)/dt^2 = \{-[d(H4)/dt]^2 A - AP \times V|V|\}/(A \times H4) \quad (1)$$

Connecting Liquid Region:

$$d/dt\ (AP \times H1 \times \rho V) = (P1 - P2)/(2L\rho) - g/\rho \quad (2)$$

Upper Liquid Region:

$$(P1 - P2)A + AP \times V|V|\rho - H3 \times \rho Ag =$$

$$d/dt[(\rho A \times H3)\ d/dt\ (H4 + H1 + 0.5H3)] \quad (3)$$

where (as in Fig. 15):

A = cross-sectional area of the vessel
AP = cross-sectional area of the connecting pipe
g = acceleration of gravity
H1 = height of the cylindrical bubble region
H2 = height of the cover-gas region
H3 = height of upper liquid slug above the bubble
H4 = height of liquid below the bubble
L = length of the connecting pipe
P1 = pressure in bubble
P2 = pressure in the cover gas
t = time
V = velocity of liquid in the connecting pipe
|V| = absolute value of V
ρ = density of the liquid
d/dt = derivative

The pressure-volume relationship for the gas regions was programmed as ρV^{γ} = const. and also by use of the method described by Kirbyik,[8] as programmed locally by A. L. Wright,[9] which makes use of materials properties equations for UO_2.

The differential equations and the physical property equations were programmed using the CSMP system.[10]

3.1.3 Some results obtained with the code

While only a few test calculations have been done with the program, the following statements can be made.

1. The periods calculated for FAST conditions with the bypass method do not appear to differ seriously from those obtained when bypass flow is neglected.
2. If the level of liquid above the bubble is sufficiently high, the bubble can exhibit a definite downward motion as the liquid underneath it is pushed into the bypass line and into the top region, as was observed with EXCOBULLE experiments.[11]
3. The inertial effect of the fluids seriously retards the upward motion of the bubble even in this frictionless model. While the effect is probably exaggerated by the "piston" geometry, this matter should be further studied for its possible significance to HCDA analysis.
4. As a side calculation built into the program, the exponent γ was estimated at about 0.98 for the saturated UO_2 vapor in the bubble. Moreover, it was found that the ratio PV/nT for the vapor in the bubble was very close to the gas constant, indicating that UO_2 vapor could be treated as a perfect gas.

3.2 Analytical Studies with the UVABUBL Code

W. P. Schuetz*

The UVABUBL code has already been introduced and discussed in previous quarterly reports. It is a code to describe heat and mass transfer from a fuel bubble in either water or sodium, mainly related to the FAST tests. Among other modifications, an option to calculate piston-type expansion processes was added to the code during the last report period. This type of expansion is more realistic than the spherical (Rayleigh) expansion if the bubble size is of the same order as the tank diameter. During the report period, the code was applied to experimental (FAST) as well as large size conditions.

A series of runs (altogether 35 runs) was performed to analyze the FAST water tests. The main purpose was to compare the piston-type expansion with the spherical (Rayleigh) expansion and to vary the bubble emissivity. The experiments are much better described by a piston-type calculation than by a spherical expansion calculation. By assuming small values for the bubble emissivity (below 0.05), the code predictions for bubble period and maximum radius agreed reasonably well with the experimental values. A sample of the results is shown in Table 10.

In one case (W135), entrainment was included in the calculations, using an entrainment constant of 1. The effects on bubble size and period were only small, compared with the case without entrainment (W134).

We also made a first attempt to run the code for the first FAST sodium test (No. 101). Two different cases were calculated. In the first

---

*Research participant, KFK Karlsruhe.

Table 10. UVABUBL calculations for FAST water test conditions[a]

UVABUBL case	Parameters				Calculated[b] results		Experimental results	
	Cover-gas pressure (MPa)	Pool temperature (K)	Entrainment constant	Bubble emissivity	R_{max} (cm)	τ (ms)	R_{max} (cm)	τ (ms)
W120	0.025	298	0	10^{-6}	20.78	152.6	18.9	173.9
W121				0.02	20.35	147.7		
W122				0.05	20.26	161.9		
W123				0.1	20.90	c		
W124				0.2	21.95	c		
W125				0.3	22.64	c		
W126	0.122	363	0	10^{-6}	13.14	57.6	13.4	87.2
W127				0.02	13.16	63.9		
W128				0.05	13.56	c		
W129				0.1	15.10	c		
W134	0.122	298	0	0.05				
W135			1	0.05	12.58	52.8	9.9	55.0

[a]A piston-type expansion was assumed in all cases. Initial bubble temperature was 4600 K.

[b]R_{max} - Maximum bubble radius. τ = bubble period.

[c]No bubble condensation within 200 ms because of water vaporization into the bubble from the bubble-water interface.

case, using a fuel mass (MF) of 17.5 g (i.e., assuming total vaporization of the test sample), the code predicted a bubble period of 34 ms, compared with 27 ms from experiment, and a maximum bubble radius of 10.3 cm. Running a second case with MF = 10 g only, the experimental period was almost exactly verified.

By introducing typical Clinch River Breeder Reactor (CRBR) boundary conditions, the code was applied for the first time to a real reactor case. Some of these conditions are fuel mass of 7500 kg, fuel temperature of 4800 K at beginning of expansion, sodium pool height of 9.9 m, and cover-gas volume of 21 m^3. In all cases, the cover-gas volume is the limiting factor for the bubble expansion. The bubble period is very sensitive to the amount of fission gas and volatile fission products assumed to participate in the expansion process.

Finally, Rayleigh-type expansion cases were run for fuel amounts on the order of 1 kg in a very large pool, where vessel wall effects could be neglected, to study buoyancy and condensation. Typically, a 1-kg and 4800-K UO_2 bubble is predicted to condense in an 800-K sodium pool within 0.8 s and rise 0.9 m during that time, if an emissivity of 0.05 is assumed. It should be pointed out, however, that the emissivity, which still is not very well known, plays a very important role in these calculations.

REFERENCES

1. T. S. Kress and M. L. Tobias, *LMFBR Aerosol Release and Transport Program Quart. Prog. Rep. for January–March 1981*, NUREG/CR-2299, Vol. 1 (NUREG/TM-7946).

2. T. S. Kress and M. L. Tobias, *LMFBR Aerosol Release and Transport Program Quart. Prog. Rep. for April–June 1981*, NUREG/CR-2299, Vol. 2 (ORNL/TM-7974).

3. T. S. Kress and M. L. Tobias, *LMFBR Aerosol Release and Tranport Program Quart. Prog. Rep. for July–September 1981*, NUREG/CR-2299, Vol. 3 (ORNL/TM-8149).

4. E. F. Losco, "Silver," chap. 40 in *Reactor Handbook*, 2d ed., vol. 1, Materials, ed. by C. R. Tipton, Jr., Interscience, New York, 1960.

5. Sandia Laboratories, *Core Melt Experimental Review*, SAND-74-0382, (August 1976).

6. Westinghouse Electric Company, *Floating Nuclear Plant Core Melt Constituents*, Atlantic Generating Station, PSAR Public Service Electric and Gas Co., Newark, New Jersey, Docket No. 50-477-478 (March 1974).

7. S. Hagen et al., *Projekt Nukleare Sicherheit*, KFK 2750, Kernforschungszentrum Karlsruhe, GmbH, Karlsruhe (November 1978).

8. M. Kirbiyik, *Fuel-Vapor Generation in LMFBR Core Disruptive Accidents*, Ph.D. Dissertation, Nuclear Engineering Department, University of Virginia, Charlottesville, Virginia, 1975.

9. A. L. Wright, personal communication.

10. International Business Machines Corp., *Continuous System Modeling Program III (CSMP III)*, Program Reference Manual SH19-7001-3, Fourth Edition (December 1975).

11. M. Amblard et al., "The EXCOBULLE Experiments on the Expansion of Large Two-Phase Bubbles," *Nucl. Eng. Des.* 61(3), 459–468 (December 1980).

NUREG/CR-2299, Vol. 4
ORNL/TM-8307
Dist. Category R7

Internal Distribution

1-4. R. E. Adams
5. R. F. Benson
6. H. W. Bertini
7. J. R. Buchanan
8. G. E. Creek
9. U. Gat
10. T. H. Hanratty (Consultant)
11. H. W. Hoffman
12. M. T. Hurst
13. T. S. Kress
14. A. L. Lotts
15. R. E. MacPherson
16. A. P. Malinauskas
17. G. W. Parker
18. J. Petrykowski
19-20. T. W. Robinson, Jr.
21. J. M. Rochelle
22. R. L. Rudman (Consultant)
23. A. M. Smith
24. I. Spiewak
25. A. L. Sutton, Jr.
26-27. M. L. Tobias
28. H. E. Trammell
29. J. L. Wantland
30. R. P. Wichner
31. G. D. Whitman
32. A. L. Wright
33. ORNL Patent Office
34. Central Research Library
35. Document Reference Section
36-37. Laboratory Records Department
38. Laboratory Records (RC)

External Distribution

39. M. Silberberg, Chief, Fuel Behavior Branch, Division of Accident Evaluation, Nuclear Regulatory Commission, Washington, DC 20555
40. R. Sherry, Division of Accident Evaluation, Nuclear Regulatory Commission, Washington, DC 20555
41-44. Director, Office of Nuclear Regulatory Research, Nuclear Regulatory Commission, Washington, DC 20555
45. Office of Assistant Manager for Energy Research and Development, DOE, Oak Ridge Operations Office, Oak Ridge, TN 37830
46. R. W. Marshall, Jr., EG&G Idaho National Engineering Laboratory, P.O. Box 1625, Idaho Falls, ID 83415
47. W. A. Spencer, EG&G Idaho National Engineering Laboratory, P.O. Box 1625, Idaho Falls, ID 83415
48. R. Curtis, Chief, Severe Accident Assessment Branch, Division of Accident Evaluation, Nuclear Regulatory Commission, Washington, DC 20555
49. J. Larkins, Severe Accident Assessment Branch, Division of Accident Evaluation, Nuclear Regulatory Commission, Washington, DC 20555
50. T. Walker, Severe Accident Assessment Branch, Division of Accident Evaluation, Nuclear Regulatory Commission, Washington, DC 20555
51-52. Technical Information Center, DOE, Oak Ridge, TN 37830
53-347. Given distribution as shown in category R7 (NTIS-10)

☆ U.S. GOVERNMENT PRINTING OFFICE: 1982-546-067/29